ORIGINAL ARTICLE

Dynamical properties of firing patterns in ELL pyramidal neuron under external electric field stimulus

Lei Wang · Shenquan Liu · Linlin Zhang · Yanjun Zeng

Abstract Pyramidal neurons in the electrosensory lateral line lobe (ELL) of weakly electric fish activate in an environment of time-varying electric fields, which are generated by the fish itself, while how these pyramidal neurons would behave or what kinds of firing patterns these neurons would produce under different electric fields is still unclear. In this research, the firing behaviors of ELL pyramidal neuron under DC and AC electric field stimulus are investigated in a two-compartment neuron model. By means of numerical simulations we show that firing patterns of the model ELL pyramidal neuron are much diverse under different values of DC electric field, and neuronal spike frequency exhibits a monotone decreasing trend with the linearly increased DC fields, moreover, the transition mode between these firing patterns with the variation of DC electric fields demonstrates an explicit periodic route. While for AC electric fields, neuronal firing frequency periodically transforms with the increase of AC frequency, particularly, a special transition pattern (from multi-period bursting to spiking) repeatedly appears with the change of AC frequency. Our simulation results indicate that ELL pyramidal neurons fire dynamically under the time-varying electric fields, the diversity of firing patterns and their periodic transition modes may imply the potential roles of these dynamical firings in the coding strategy of sensory information processing.

Keywords ELL pyramidal neuron · Electric field · Firing patterns · Two-compartment model · Spike frequency · Interspike interval (ISI)

Introduction

Bursting is an extraordinary dynamical phenomenon embedded in the spike trains of many neurons, in which a neuron periodically switches from a cluster of densely fired spikes to quiescent state and back again [1, 2]. Burst firing has been recognized to play a significant role in neuronal information processing [3], and it was also thought to have functional effects in reliable signaling [4] and neuronal synaptic plasticity [5]. Due to its dynamical complexity and physiological significance in neural signal encodings, several typical bursting types have been indentified and analyzed using the method of fast/slow analysis, e.g., triangular [6], square-wave [7], parabolic [8] and elliptic [9]. Recently, a novel bursting type was found in the electrosensory lateral line lobe (ELL) pyramidal cells of the weakly electric fish, *Apteronotus Leptorhynchus*, named *Ghostbursting* [10]. The ELL of weakly electric fish was recognized as the sole nucleus which can receive direct input from peripheral electroreceptor afferents, and it was also the primary processing centre for electric information [11]. In the ELL, weakly electric fishes can acquire information from their living surroundings by detecting the spatial–temporal patterns of electric potential over their skin, produced by perturbations in a self-generated electric

L. Wang · S. Liu (✉)
Department of Mathematics, South China University of Technology, 510640 Guangzhou, China
e-mail: mashqliu@scut.edu.cn

Present Address:
L. Wang
School of Biomedical Enginerring, Shanghai Jiao Tong University, 200240 Shanghai, China

L. Zhang · Y. Zeng (✉)
Biomedical Engineering Center, Beijing University of Technology, 100022 Beijing, China
e-mail: yjzeng@bjut.edu.cn

field [12]. The field disperses in the fish's living environment, and can be perceived by both the emitting fish and other nearby fishes. The electric fish uses electroreceptors on their skin to detect the field, which then transmit signals to pyramidal neurons in the ELL; consequently, the pyramidal neurons participate in the primary sensory information processing in the pathway from the periphery to the brain of the fish [13].

Since it was found, ghostbursting of ELL pyramidal neuron has been subject to intensive research owing to their potential roles in the coding strategy of sensory information. Doiron et al. [10] investigated the influence of external dc stimulus and potassium ion conductance in the dendritic compartment on the ghostbursting behaviors of ELL pyramidal neuron. Subsequently, the effects of varying both the conductance between the somatic and dendritic compartments, and the ratio of somatic to whole-cell areas in the model were analyzed, and found that all of these parameters have strong impacts on the ghostbursting patterns [14]. Furthermore, firing properties of the model ELL pyramidal neuron under periodic forcing were studied [13], their numerical results showed that sinusoidal modulation of the current injected into the model can switch it from periodic spiking to burst firings, or vice versa, depending on the frequency of modulation. There are still some researchers examining the synchronous activity of coupled ghostburster neurons [15].

For the living surroundings in which the ELL pyramidal neuron activate is diffused with electric fields, thus, the ghostbursting behaviors of ELL pyramidal neuron must be influenced with the variation of electric fields. A previous numerical study on the firing patterns of modified Hodgkin-Huxley neuron under external sinusoidal electric fields showed that the model neuron can display a rich variety of firings by the modulation of electric field, and the interspike interval (ISI) sequences have a much diverse variation [16]. Experimental observation on CA3 pyramidal neuron indicated that the sensitivity of coherent oscillations in rat hippocampus under DC and AC electric field was much different. For DC electric field, it can alter the membrane potential in CA3 pyramidal neuron by 0.18 mV per Vm^{-1}, while AC electric field had relatively smaller effects on the membrane potentials, and the sensitivity decreased as an exponential decay function of the AC frequency [17].

ISI which measure the time difference between adjacent peaks in neuronal spike trains, have been assumed to be an effective approach in characterizing the dynamical properties and complex bifurcation structures in neuronal firings, and method for acquiring the values of ISI was described detailedly in [18]. In the following study, we investigated the ghostbursting patterns under DC and AC electric field forces, and we also analyzed the neuronal spike frequency and the ISI bifurcation diagrams which can characterize the transitions

between different firing patterns with the variation of the amplitude of DC fields and the frequency of AC fields.

Model and method

The model neuron we studied in this paper is a two-compartment model of ELL pyramidal neuron [13]. The fast inward Na^+ currents and outward delayed rectifying (Dr) K^+ currents are both contained in the somatic compartment and dendritic compartment, termed as $I_{Na,s}$, $I_{Na,d}$, $I_{Dr,s}$ and $I_{Dr,d}$, respectively.

The mathematical descriptions of this model pyramidal neuron are the following equations:

$$C_m \frac{dV_s}{dt} = I_s - g_{Na,s} \cdot m_{\infty,s}^2(V_s) \cdot (1 - n_s) \cdot (V_s + V_E - V_{Na}) - g_{Dr,s} \cdot n_s^2 \cdot (V_s + V_E - V_K) - g_{leak} \cdot (V_s + V_E - V_l) + \frac{g_c}{k} \cdot (V_d - V_s)$$

(1)

$$\frac{dn_s}{dt} = \frac{n_{\infty,s}(V_s) - n_s}{\tau_{n,s}}$$

(2)

$$C_m \frac{dV_d}{dt} = - g_{Na,d} \cdot m_{\infty,d}^2(V_d) \cdot h_d \cdot (V_d + V_E - V_{Na}) - g_{Dr,d} \cdot n_d^2 \cdot p_d \cdot (V_d + V_E - V_K) - g_{leak} \cdot (V_d + V_E - V_l) + \frac{g_c}{1 - k} \cdot (V_s - V_d)$$

(3)

$$\frac{dh_d}{dt} = \frac{h_{\infty,d}(V_d) - h_d}{\tau_{h,d}}$$

(4)

$$\frac{dn_d}{dt} = \frac{n_{\infty,d}(V_d) - n_d}{\tau_{n,d}}$$

(5)

$$\frac{dpd}{dt} = \frac{p_{\infty,d}(V_d) - p_d}{\tau_{p,d}}$$

(6)

The values correspond to the model parameters introduced in Eqs. (1–6) are provided in Table 1, which are adopted from Ref. [13]. The activation function of gating variables follows the expression below.

$$x_{\infty,s(d)}(V_{s(d)}) = \frac{1}{1 + e^{-(V_{s(d)} - V_{1/2})/K}} \quad (x = n_s, h_d, n_d, p_d)$$

(7)

Other parameters can be found in Ref. [13].

The external electric field stimulus conducts the following form:

$$V_E = A + B \sin(wt)$$

(8)

When $B = 0$, the electric field V_E is a DC form, while $A = 0$ makes the V_E a AC form.

Altogether the model consists of six differential equations. Simulations were performed using the MATLAB

Table 1 Parameter values for the ghostbursting model neuron

Current	g_{max}	$V_{1/2}$	K	τ
$I_{Na,s}(m_{\infty,s}(V_s))$	55	−40	3	–
$I_{Dr,s}(n_s(V_s))$	20	−40	3	0.39
$I_{Na,d}(m_{\infty,d}(V_d)/h_d(V_d))$	5	−40/−52	5/−5	–/1
$I_{Dr,d}(n_d(V_d)/p_d(V_d))$	15	−40/−65	5/−6	0.9/5

software, and the fourth-order Runge–Kutta algorithm was employed to calculate the values of membrane potential with time step being 0.01 ms.

Simulation results

Firing sequences of action potential in the ghostburster neuron

Action potential as a characterization of the electrical activity of neurons, it can reflect and encode the features of neuronal activity in a large extent. The ghostbursting patterns produced by the model neuron in this paper were presented in Fig. 1. From the figure we can see, both the soma and the dendrite of the neuron were found to be capable of generating action potentials, and spike numbers in each burst were also clearly depicted. As the potassium

inactivation in the dendritic compartment (p_d) was critical in the initiation of ghostbursting, we drew the diagram of p_d with respect to the somatic action potential V_s, which was illustrated in Fig. 1d. From Fig. 1d, we can easily observe the period numbers or spike numbers in each burst. For example, in Fig. 1a, the somatic compartment showed a period-5 ghostbursting pattern, while the number of cycles in Fig. 1d was precisely five. Thus, in the following analysis, diagrams similar with Fig. 1d were used to describe the period number of their corresponding ghostbursting behaviors.

Variation of ghostbursting patterns under DC electric field stimulus

When the amplitude of DC electric field linearly increased, ghostbursting patterns of the model neuron underwent a periodic variation trend. As shown in Fig. 2, the ghostbursting behavior exhibited a period-1 pattern when $A = -28$. When A increased to -10, the neuron fired a period-2 pattern, and a period-4 pattern occurred when A increased to -6, this transition of period number from one to two and four was apparently a period-doubling bifurcation phenomenon, which could also be observed in the ISI bifurcation diagram of Fig. 3b. After the period-doubling cascade, the model neuron entered into a chaotic firing pattern when $A = -4.8$, after that, a period-3 firing pattern
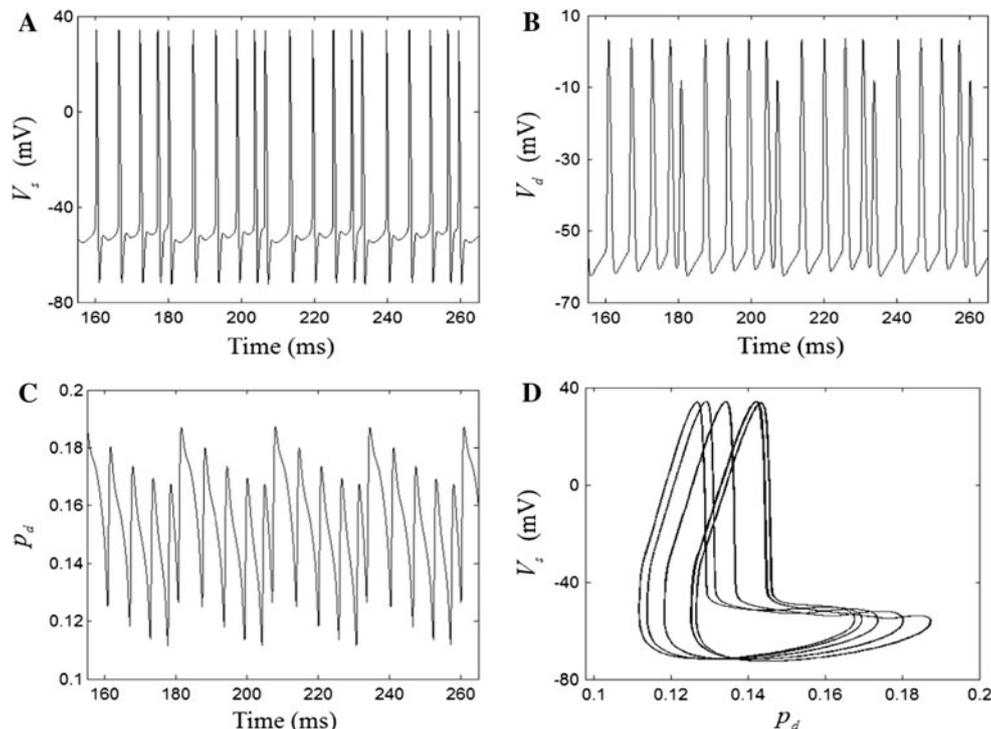

Fig. 1 Ghostbursting patterns in the model neuron. **a** Action potential of the somatic compartment; **b** action potential of the dendritic compartment; **c** time course of the gating variable p_d; **d** diagram of p_d versus V_s
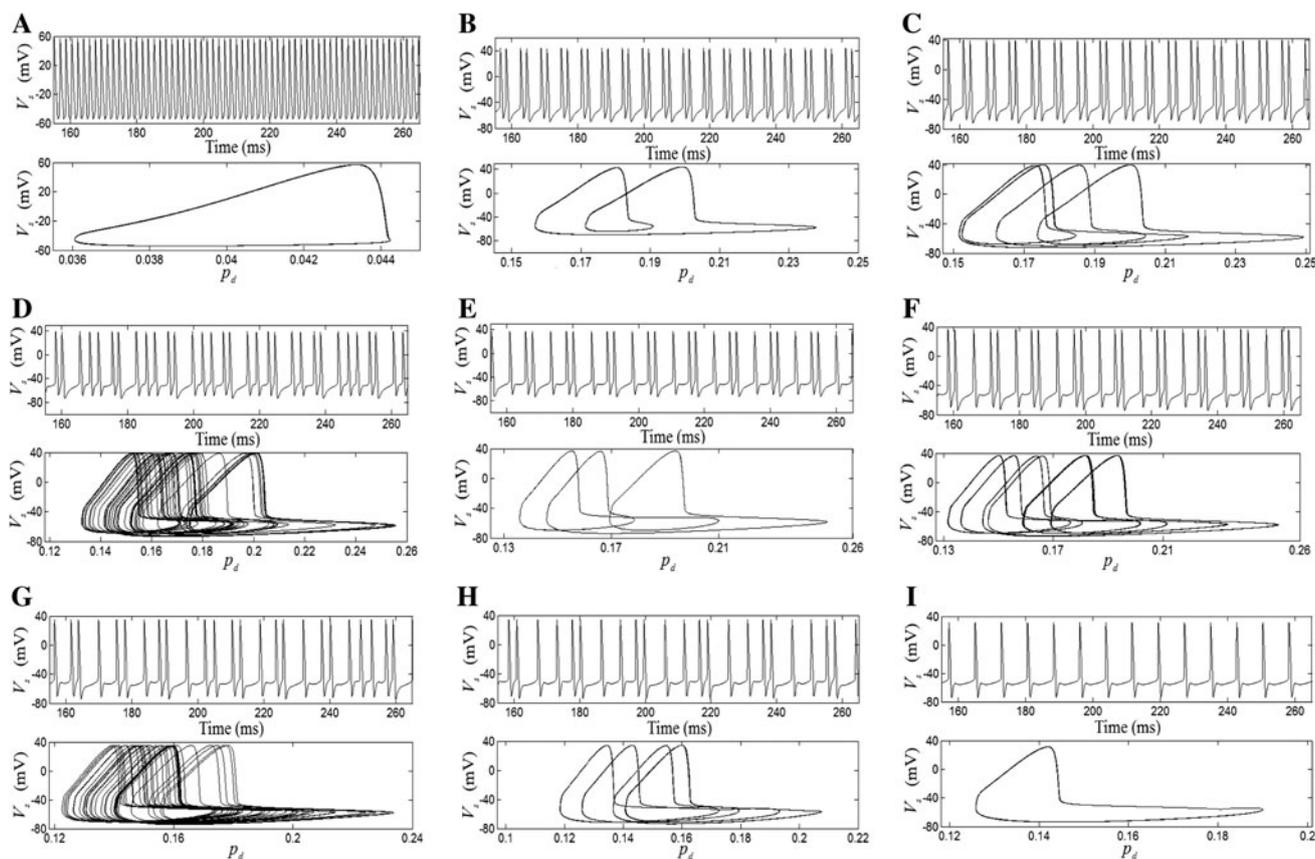
Fig. 2 Somatic action potentials and the corresponding firing periods under different values of A. From **a–i**, the value of A is −28, −10, −6, −4.8, −3, −2.5, −1, 0, 3 (mV), respectively. In each diagram, the *upper part* represents the somatic action potentials similar to Fig. 1a, and the *lower part* indicates the corresponding firing number the model neuron behaved, similar to Fig. 1d. Different values of A can induce different ghostbursting patterns and firing numbers

Fig. 3 Spike frequency and ISI bifurcation diagram with the variation of A. **a** Spike frequency; **b** ISI diagram
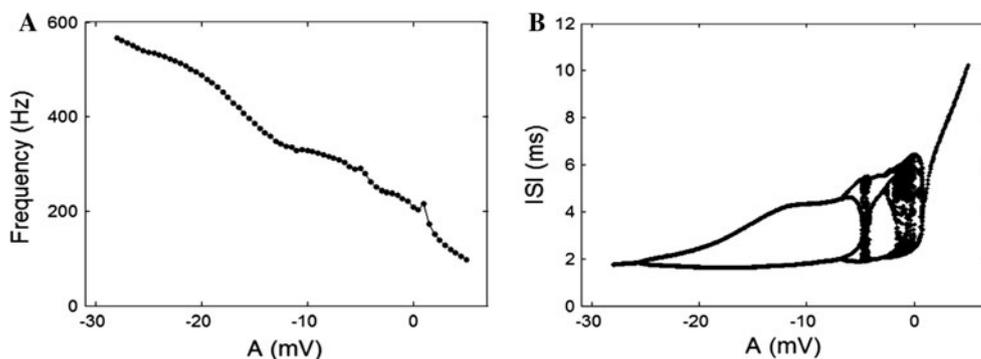
appeared when A continued to increase, following that was a period-6 firing pattern. Again, the chaotic firing emerged when A reached −1, and finally, the model neuron displayed a period-1 ghostbursting pattern through a period-4 pattern.

The detailed transition modes between these firing patterns with the linear increase of DC electric field was illustrated in Fig. 3b, which can clearly depict how these firing patterns switch from one to another. We also gave the variation of neuronal spike frequency with the change of DC electric field in Fig. 3a, which indicated that for larger negative DC electric field, neural firing frequency was rather higher, however, when A linearly increased from −28 to 5, the frequency decreased monotonously, which suggested that firing frequency of the model pyramidal neuron can be modulated by external DC electric field.
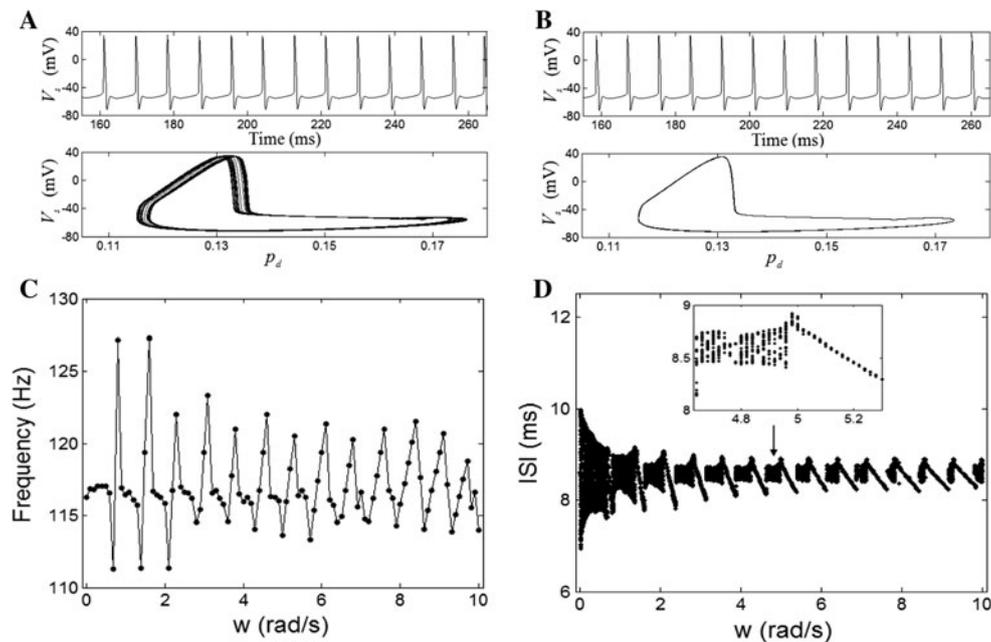
Fig. 4 Analysis of the ghostbursting behavior of ELL pyramidal neuron under AC electric field stimulus. **a**, **b** denote the somatic action potentials and the corresponding firing periods under different values of w, the value of w is 4.8, 5.2 (rad/s), respectively; **c** spike frequency; **d** ISI diagram

Variation of ghostbursting patterns under AC electric field stimulus

In this section, we assumed that the variation of external electric field has a sinusoidal form which was different from the linear form in "Variation of ghostbursting patterns under DC electric field stimulus". In Fig. 4, we gave two examples of the ghostbursting pattern under two different values of AC frequency w, Fig. 4a manifested a multi-period bursting pattern, while Fig. 4b presented a simple period-1 pattern.

The variation of neuronal spike frequency and the transition modes between different firing patterns with the change of w were demonstrated in Fig. 4c, d. In Fig. 4c, the neuronal firing frequency showed a periodic change when w increased from 0 to 10, although the period cycle was not always exactly the same. This variation trend was completely different from the monotonous trend shown in Fig. 3a.

Figure 4d illustrated the ISI bifurcation diagram which characterizes the transition between different ghostbursting patterns, from this diagram, we got that a special transition pattern (from multi-period bursting to regular spiking, shown in the insert figure) periodically appeared with the increase of w. This periodic variation phenomenon may imply some potential roles in sensory information encodings.

Conclusions

By determining the exact mechanisms of various firing patterns, one can gain insight into a plenty of spiking behaviors and the nature of transition modes between them. This understanding can promote and deepen the investigation of how different factors might influence neuronal firing patterns [19]. In this study, the firing behaviors of ELL pyramidal neuron in weakly electric fish, *Apteronotus Leptorhynchus* under DC and AC electric field were analyzed. Our modeling results manifested that a variety of periodic ghostbusrting patterns were observed under different amplitudes of the DC electric field (Fig. 2), and the transition between these firing patterns showed a clear periodic route when DC electric field increased from −28 to 5 (Fig. 3b), in addition, the firing frequency of the ghostburster neuron exhibited a monotonous decreasing trend with the linearly increased DC field (Fig. 3a). While for AC electric field stimulus, firing patterns with multi-period bursting and regular spiking in the model neuron repeatedly occurred and switched between each other with the increase of AC frequency (Fig. 4d), and the neuronal spike frequency also showed a quasi-periodic variation (Fig. 4c). These diverse spiking patterns that the ghostburster neuron produced under the time-varying electric field and distinctions between the dynamical transition routes and neuronal firing frequency under DC and AC

electric field may insinuate some potential mechanisms in the coding strategy of sensory information processing of the electric fishes.

References

1. Lisman JE (1997) Bursts as a unit of neural information: making unreliable synapses reliable. Trends Neurosci 20(1):38–43
2. Laing CR, Longtin A (2002) A two-variable model of somatic-dendritic interactions in a bursting neuron. Bull Math Biol 64(5):829–860
3. Izhikevich EM, Hippensteadt F (2004) Classification of bursting mappings. Int J Bifurcat Chaos 14(11):3847–3854
4. Eyherabide HG, Rokem A, Herz AV, Samengo I (2009) Bursts generate a non-reducible spike-pattern code. Front Neurosci 3(1):8–14
5. Wang XJ (1999) Fast burst firing and short-term synaptic plasticity: a model of neocortical chattering neurons. Neuroscience 89(2):347–362
6. Rush ME, Rinzel J (1994) Analysis of bursting in a thalamic neuron model. Biol Cybern 71(4):281–291
7. Sherman A, Rinzel J (1992) Rhythmogenic effects of weak electrotonic coupling in neuronal models. PNAS 89(6):2471–2474
8. Rinzel J, Lee YS (1987) Dissection of a model for neuronal parabolic bursting. J Math Biol 25(6):653–675
9. Av-Ron E, Parnas H, Segel LA (1993) A basic biophysical model for bursting neurons. Biol Cybern 69(1):87–95
10. Doiron B, Laing C, Longtin A, Maler L (2002) Ghostbursting: a novel neuronal burst mechanism. J Comput Neurosci 12(1):5–25
11. Berman NJ, Maler L (1999) Neural architecture of the electrosensory lateral line lobe: adaptations for coincidence detection, a sensory searchlight and frequency-dependent adaptive filtering. J Exp Biol 202:1243–1253
12. Kelly M, Babineau D, Longtin A, Lewis JE (2008) Electric field interactions in pairs of electric fish: modeling and mimicking naturalistic inputs. Biol Cybern 98(6):479–490
13. Laing CR, Longtin A (2003) Periodic forcing of a model sensory neuron. Phys Rev E 67(5):051928
14. Laing CR, Doiron B, Longtin A, Maler L (2002) Ghostbursting: the effects of dendrites on spike patterns. Neurocomputing 44–46:127–132
15. Sun L, Wang J, Deng B (2009) Global synchronization of two ghostburster neurons via active control. Chaos Solitons Fractals 40(3):1213–1220
16. Han CX, Wang J, Deng B (2009) Fire patterns of modified HH neuron under external sinusoidal ELF stimulus. Chaos Solitons Fractals 41(4):2045–2054
17. Deans JK, Powell AD, Jefferys JG (2007) Sensitivity of coherent oscillations in rat hippocampus to AC electric fileds. J Physiol 583(2):555–565
18. Wang L, Liu S, Zhang J, Zeng Y (2012) Burst firing transitions in two-compartment pyramidal neuron induced by the perturbation of membrane capacitance. Neurol Sci 33(3):595–604
19. Kepecs A, Wang XJ (2000) Analysis of complex bursting in cortical pyramidal neuron models. Neurocomputing 32–33:181–187